Chapter 25

Microfibrous Entrapped ZnO–Support Sorbents for High Contacting Efficiency H_2S Removal from Reformate Streams in PEMFC Applications

Y. Lu, N. Sathitsuksanoh, H. Y. Yang, B. K. Chang, A. P. Queen, and B. J. Tatarchuk

Center for Microfibrous Materials Manufacturing, Department of Chemical Engineering, Auburn University, Auburn, AL 36849

A sintered microfibrous carrier consisting of 2.0 - 3.0 vol% of 4 and 8 μm (dia.) Ni fibers is utilized to entrap from 20 to 30 vol% of 150-250 μm (dia.) carbon and SiO_2 support particulates. Zinc oxide is then placed onto the supports by impregnation at loadings ranging from 15 to 20 wt%. Two different sorbent recipes have been developed. ZnO/Carbon entrapped material for low temperature use is envisioned to operate as a last line of defense at stack temperatures. ZnO/SiO_2 entrapped material is employed for regenerable use in a continuous batch mode at ca. 400°C to scavenge bulk H_2S. The nano-dispersed nature of ZnO combined with the use of small support particulates promotes high ZnO utilization, high contacting efficiency, and high accessibility of ZnO. At equivalent bed volumes, microfibrous entrapped sorbents provide 2- to 3-fold longer breakthrough time for H_2S (with a 67% reduction in sorbent loading), compared to packed beds of commercial 1-2 mm extrudates. Five-log reductions in H_2S concentration with up to 67% ZnO utilization at breakthrough are achieved. Hydrogen sulfide concentrations from 50 ppmv (up to 20,000 ppmv) can be reduced to as little as 0.1 ppmv (at R.T.) and 0.6 ppmv (at 400°C) in 30% H_2O at face velocities of 1.2-1.7 cm/s for layers as thin as 1.0 mm. Regenerability in

In Microreactor Technology and Process Intensification; Wang, Y., et al.;
ACS Symposium Series; American Chemical Society: Washington, DC, 2005.

air at 500-600°C is also facilitated by the nano-dispersed nature of the ZnO and the use of small support particulates. The recovery percentage of ZnO utilization using microfibrous entrapped sorbents is up to 5-fold higher than that for packed beds of 1-2 mm commercial extrudates. Furthermore, composite beds consisting of packed beds of large extrudates (ca. 1-2 mm dia.) followed by the above noted microfibrous entrapped sorbents as polishing layers has been demonstrated with a great extension in gas life. This approach synergistically combines the high volume loading of packed beds and the overall contacting efficiency of small particulates.

Proton-exchanged membrane fuel cells (PEMFC) for power systems have become the focus of significant interest. A recent challenge confronting these efforts is the development of on-board fuel processing technologies utilizing high energy density commercial-grade hydrocarbon fuels. The bed utilization efficiency as well as overall system weights and volumes are indeed very important fuel processor design considerations. Traditional approaches such as packed beds of 1-5 mm (dia.) catalysts and/or sorbents normally suffer from high intraparticle mass/heat transfer and low contacting efficiency. In those cases larger amount of catalysts and/or sorbents than necessary are needed for meeting the fuel cell requirements, which in turn result in low bed utilization efficiency while increasing overall system weight and volume. Sintered microfibrous media developed at Auburn University have substantial potential for enhanced heat/mass transfer, improved contacting efficiency and regenerability (*1-9*). This generic approach utilizes a high void volume and tailorable microfibrous carrier, with high contacting efficiency, to entrap micro-sized sorbent and/or catalyst particulates. Use of these materials allows reduction of both reactor weight and volume while permitting development of small and robust fuel processors. Microfibrous entrapped 16% Ni/Al_2O_3 catalysts for toluene hydrogenation in a trickle bed reactor have demonstrated 2-6 times higher specific activities than conventional packed bed catalysts on a gravimetric basis, while volumetric activities of 40 vol% composite catalysts were 80% higher than conventional extrudates (*8*). Microfibrous entrapped 1% $Pt\text{-}M/Al_2O_3$ for PrOx CO provided 3-fold higher or more bed utilization efficiency compared to packed beds of 2-3 mm (dia.) pellets (*10, 11*) at same CO conversion. Two-phase mass-transfer

testing indicated that microfibrous composite catalysts take advantage of both high gas-liquid contacting and bulk mixing at low pressure drop with the potential to provide enhanced catalyst utilization (*12*). Additionally, the microfibrous media can be made into thin sheets of large area and/or pleated to control pressure drop and contacting efficiency. The fabrication of the microfibrous media is based on reliable, proven, high-speed, roll-to-roll, papermaking and sintering processes, substantially reducing production costs while improving product quality.

Hydrogen sulfide removal is a key step in ensuring the activity maintenance of various fuel processing catalysts and high value membrane electrode assemblies. For achieving maximum useful life of the PEMFCs, it is crucial to reduce H_2S concentration less than 0.1 ppmv (*13, 14*). Zinc oxide is well known as a highly efficient desulfurizer due to extremely low equilibrium H_2S concentration and is widely used for sulfur removal from various gas streams. Normally, packed beds of large ZnO sorbent extrudates with high sorbent inventory, are employed to scavenge H_2S from reformate streams for fuel cell applications (*15*). Large particles result in low ZnO utilization and poor regenerability because of low contacting efficiency, and intraparticle and lattice diffusion limits (*16*).

In this work, a microfibrous carrier consisting of 2.0-3.0 vol% of 4 and 8μm (dia.) Ni fibers was utilized to entrap 150-250 μm ZnO/Carbon and ZnO/SiO_2 H_2S sorbents. ZnO/Carbon for low temperature use is envisioned to operate as a last line of defense at stack temperatures. ZnO/SiO_2 for regenerable use is employed to scavenge bulk H_2S from reformate streams in a continuous batch mode at ca. 400°C. Up to 30 vol% H_2O in reformate streams is required to perform downstream WGSRs, and to keep membrane electrode assemblies from drying. Thermo-dynamic data indicates that H_2S concentration in 30% H_2O is 0.6ppmv at 400°C but can be reduced to less than 0.1 ppmv when temperature is below 200°C (*16*). That is why two different ZnO/support recipes were developed. Composite beds consisting of packed beds of 1-2 mm (dia.) commercial extrudates followed by high contacting efficiency microfibrous entrapped polishing sorbents were also demonstrated, providing a great extension of gas life.

Experimental

Preparation of Microfibrous Entrapped ZnO/Support Sorbents

Sintered microfibrous carrier was used to entrap 150-250 μm diameter support particulates first by regular wet layer paper-making/sintering procedure (*1-8*), where SiO_2 (300 m^2/g, Grace Davison), BPL activated carbon (560 m^2/g, Calgon), and γ-Al_2O_3 (220 m^2/g, Alfa Aesar) were chosen as the supports. ZnO

was then placed onto the supports by incipient wetness impregnation. Detailed procedure is described in a sample preparation: 7.5 g of 8 μm Ni fibers, 2.5 g of 4 μm Ni fibers, and 2.5 g of cellulose were added into water and stirred vigorously to produce a uniform suspension. The produced suspension and 18 g of 150-250 μm SiO_2 were added into the headbox of the 1.0 ft^2 M/K sheet former under aeration. 1.0 ft^2 preform was then formed by vacuum filtration followed by drying on a heated drum. Said preform was pre-oxidized in air flow for 2 h at 500°C followed by sintering in H_2 flow for 1 h at 900°C. As-prepared microfibrous entrapped SiO_2 was immersed into a ZnO sol for 10 min, and subsequently vacuum drained, calcined in air for 30 min at each temperature point of 80°C, 100°C, 120°C, 140°C, 160°C, 180°C. The ZnO sol was prepared by adding 70 ml $NH_3 \cdot H_2O$, 42 g $(NH_4)_2CO_3$, and 66 g $Zn(Ac)_2 \cdot 6H_2O$ in series into 56 ml water under vigorous stirring.

The composition and physico-chemical properties of as-prepared micro-fibrous entrapped ZnO/support sorbents are summarized in Table I. A commercial ZnO sorbent (3/16" pellet, 25 m^2/g, 90 wt% ZnO) from Sud Chemie and several carbon-based sorbents for respiratory cartridge use from the manufactures of MSA, 3M, Scott, and Willson, were crushed and sieved into desired particle size for comparative study use.

It should be noted that by utilizing the wet layer paper-making/sintering process, the particulate sizes of 150-250 μm can be entrapped and the uniform dispersion of the particulates within the fibrous matrix can be obtained. However, the different particulate sizes used result in different settling rate of the particulates during the wet layer paper-making process, which causes an ununiform dispersion of the particulates within the microfibrous structure. The well dispersed particulates throughout the microfibrous network is desired to avoid bypassing.

Table I. Composition, physico-chemical properties of microfibrous entrapped ZnO/support sorbents

Microfibrous sorbent	*ZnO*	*Support*		*Ni fiber*		*Voidage (%)*
	wt%	*wt%*	*vol%*	*wt%*	*vol%*	
ZnO/SiO_2	18[a]/17.3[b]	43	25	39	2	73
ZnO/Carbon	19[a]/18.6[b]	44	28	37	2	70
$ZnO/\gamma\text{-}Al_2O_3$	18[a]	43	24	39	2	74

[a] By weighing; [b] ICP-AES analysis results, carried out on a Thermo Jarrell Ash ICAP 61 Simultaneous Spectrometer.

Micro-Reactor Evaluation and Characterization

Hydrogen sulfide pulse reactions were carried out in a quartz tube reactor (i.d. 4 mm) system equipped with an online GC using a TCD. 0.11 g microfibrous entrapped ZnO/SiO_2 sorbent and 0.022 g Sud-Chemie extrudates were used with a constant ZnO loading (0.02 g), respectively. Hydrogen sulfide (50 μL) was pulsed every 2 min using H_2 (30 mL) as carrier gas. Absorption with an H_2S challenge of 50 ppmv in a model reformate (40% H_2, 10% CO, 20% CO_2, 30% N_2, BOC GASES) was carried out at 400°C or stack temperatures (R.T.-100°C) at a face velocity of 1.7 cm/s. Sorbent loading was kept constant at 0.29 mL (11 mm dia. × 3 mm thick).

Absorption/regeneration cycle test and regenerability comparison were carried out using 2 vol% H_2S in H_2 as feedgas. Sorbent loading was kept constant at 0.9 mL(7 mm dia. × 15 mm thick). Absorption was performed at 400°C at face velocity of 1.2 cm/s. Regeneration was performed at 500-600°C in an air flow (50 ml/min) for 1-3 h.

The composite bed consisting of a packed bed (7 mm dia. × 7 mm thick) of Sud-Chemie extrudates (1-2 mm) followed by a polishing sorbent layer (3 mm in thickness) was tested at face velocity of 1.2 cm/s using 2 vol% H_2S in H_2 as feedgas at 400°C. The outlet H_2S concentrations were determined by an online GC with TCD combined with lead acetate strip and a MultiRAE Plus multigas monitor (PMG-50/5P). One ppmv outlet H_2S concentration was defined as breakthrough. H_2S concentrations from 50 ppmv to 2.0 vol% were reduced to as little as thermodynamic equilibrium values (0.6 ppmv at 400°C and less than 0.1 ppmv at R.T. to 100°C in 30% H_2O).

Powder XRD patterns were recorded on Rigaku instrument using a scanning speed of 4°/min and an accelerating voltage of 40 kV. SEM measurements were carried out using a Zeiss DSM 940 instrument.

Results and Discussion

Characteristics of Microfibrous Entrapped ZnO/SiO_2 and ZnO/Carbon

SEM micrographs in Figure 1 show microstructures of the thin microfibrous entrapped ZnO/SiO_2 and ZnO/Carbon sorbents for H_2S absorption, respectively. ZnO/support particulates of 150-250 μm were uniformly entrapped into a well sinter-locked 3-dimensional network of 8 and 4 μm nickel fibers. Use of small particulate can significantly attenuate the intraparticle diffusion limit and allow high contacting efficiency with gas streams. XRD patterns in Figure 2 show that the mixtures of ZnO and supports with comparable composition with the corresponding ZnO/support sorbents afforded very strong and narrow peaks

assigned to large ZnO crystals. In comparison, both ZnO/Carbon and ZnO/SiO_2 entrapped materials afforded very weak and broad XRD peaks of ZnO. Zinc oxide crystal size for both SiO_2- and Carbon-supported sorbents is determined to be <5 nm, 2-fold smaller than that for Sud-Chemie extrudates (ZnO crystal size: 15 nm). This reduction in ZnO crystal size can eliminate the lattice diffusion limit. Surface areas were determined to be 250 m^2/g for ZnO/SiO_2 and 360 m^2/g for ZnO/Carbon by N_2-BET. The above results indicate that the 5 nm ZnO was highly dispersed on the entrapped SiO_2 and activated carbon supports, allowing for extremely high accessibility of ZnO. In contrast the N_2-BET surface area is around 25 m^2/g for Sud-Chemie ZnO sorbent extrudates. This suggests that most of ZnO crystals are buried inside the bulk, which in turn causes poor accessibility of ZnO.

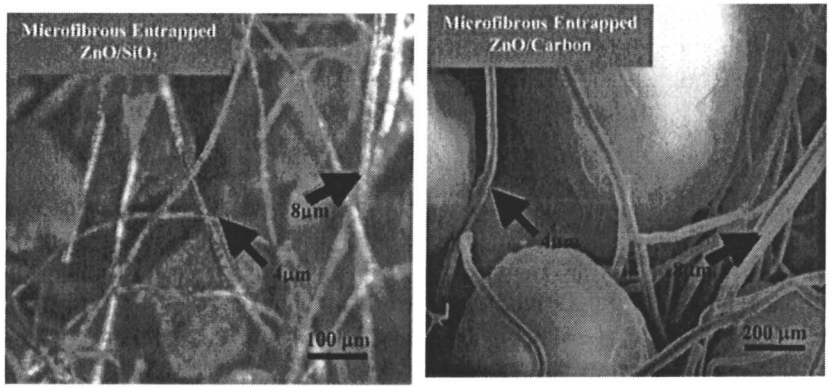

Figure 1. SEM micrographs of microfibrous entrapped ZnO/support sorbents.

Performance of Microfibrous Entrapped ZnO/SiO_2 for Regenerable Use

H_2S Pulse Reaction at 400°C

Figure 3 shows H_2S pulse reaction results over microfibrous entrapped ZnO/SiO_2 and Sud-Chemie ZnO sorbent extrudates at 400°C. At equivalent ZnO loading (0.02 g), 150-250 μm ZnO/SiO_2 entrapped materials and 150-250 μm Sud-Chemie ZnO sorbent extrudates provided higher ZnO utilization with sharp breakthrough curves, compared to ~1 mm Sud-Chemie ZnO sorbent extrudates. It is well known that H_2S adsorption reaction is a mass transfer controlled process with both intraparticle and lattice diffusion limitations (*16*). As a result, the use of small sorbent particulates significantly attenuates the intraparticle diffusion limit while providing high contacting efficiency. For Sud-Chemie ZnO sorbent, reduction of particulate size from ~1 mm to 150-250 μm results in 2.5-

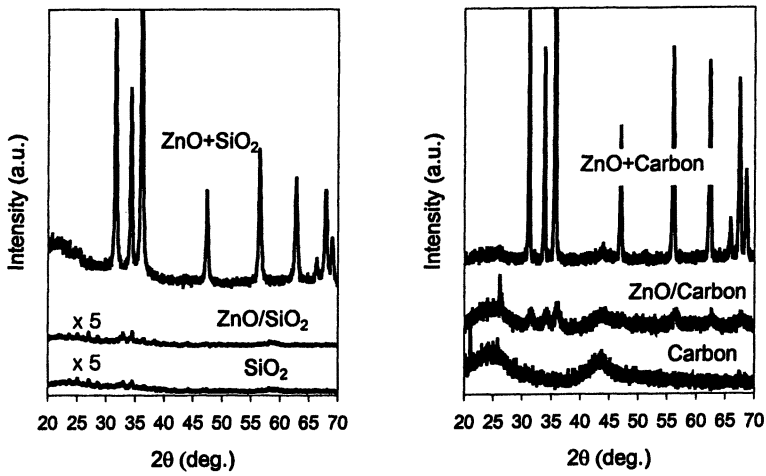

Figure 2. XRD patterns of microfibrous entrapped ZnO/SiO_2 and ZnO/Carbon.

fold difference in ZnO utilization (Utl.) while making the breakthrough curve sharper. In comparison with 150-250 μm Sud-Chemie extrudates, the nano-dispersed nature and high accessibility of the ZnO using microfibrous entrapped 150-250 μm ZnO/SiO_2 sorbents results in another 22% increase in ZnO utilization with an even sharper breakthrough curve.

H_2S Absorption in Continuous Batch Mode at 400°C in 30% H_2O

The size reduction of commercial ZnO sorbents does show the higher in removal capability and utilization efficiency. However, it should be noted that the size reduction of the commercial ZnO sorbents is not achievable in the fuel processing systems due to the issues of high pressure drop and potential fouling. These drawbacks can be overcome by utilizing the high-void nature of microfibrous carrier. Therefore, the comparison throughout will be made between microfibrous materials and packed beds of commercial 1-2 mm extrudates. Table II compares microfibrous entrapped ZnO/SiO_2 with 1-2 mm Sud-Chemie ZnO extrudates for H_2S removal from model reformate at 400°C and face velocity of 1.7 cm/s in 30% H_2O. As expected, the nano-dispersed nature and high accessibility of the ZnO combined with high contacting efficiency using microfibrous entrapped ZnO/SiO_2 promotes high ZnO utilization, compared to packed beds of 1-2 mm commercial extrudates. At equivalent bed volume (0.29 mL, 11 mm dia. x 3mm thick), microfibrous entrapped ZnO/SiO_2 (150-250 μm) provided about 2-fold longer breakthrough times for H_2S at breakthrough with about 67% reduction of sorbent loading. ZnO

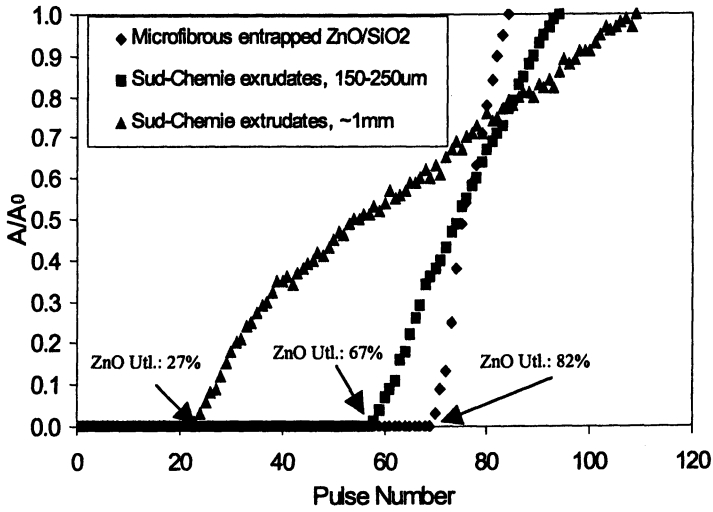

Figure 3. H_2S pulse reaction results of microfibrous entrapped ZnO/SiO_2 and Sud-Chemie ZnO sorbent extrudates at 400°C.

utilization using microfibrous entrapped ZnO/SiO_2 sorbents was 57%, 13-fold higher than that of 1-2 mm commercial extrudates.

Table II. Comparison of microfibrous entrapped ZnO/SiO_2 with Sud-Chemie ZnO sorbent extrudates for H_2S removal from model reformate at 400°C in the presence of 30% H_2O *

Sorbent	*Microfibrous entrapped ZnO/SiO_2*	*Sud-Chemie extrudates (1-2mm)*
Weight (g)	0.12	0.30
Volume (mL)	0.29	0.29
Bed thickness (mm)	3	3
Breakthrough time @1ppmv H_2S detection limit (h)	12	4.5
ZnO Utilization (%)	57	4

* Face velocity:1.7 cm/s @ 50 ppmv H_2S in model reformate (40% H_2, 10% CO, 20% CO_2, and 30% N_2); dry gas flow rate: 100 mL/min (STP).

Regenerability of Microfibrous Entrapped ZnO/SiO_2

Table III compares the regenerability of microfibrous entrapped ZnO/SiO_2 sorbents with 1-2 mm Sud-Chemie extrudates. H_2S absorption was carried out at 400°C and face velocity of 1.2 cm/s in the absence of H_2O. Clearly, the nano-dispersed nature of the ZnO combined with the use of small SiO_2 particulates also facilitates the regeneration in air. At equivalent bed volume, after regenerating at 550-600°C for 1-3 h, ZnO utilization decreased from 67% to 32-60% for microfibrous entrapped ZnO/SiO_2 and decreased from 33% to 4-20% for 1-2 mm Sud-Chemie extrudates, respectively. Under comparable regeneration conditions, the recovery percentage of ZnO utilization using microfibrous entrapped ZnO/SiO_2 is up to 10-fold higher than that of 1-2 mm Sud-Chemie extrudates. Table III also shows that microfibrous entrapped ZnO/γ-Al_2O_3 exhibited very poor regenerability compared to microfibrous entrapped ZnO/SiO_2. XRD results show that ZnO crystal size increased significantly on ZnO/γ-Al_2O_3 entrapped materials during regeneration in air at 550-600°C. Furthermore, new XRD peaks assigned to $ZnAl_2O_4$ spinel were clearly observed after regenerating at 600°C for 3 h. In comparison, ZnO crystal size increased slightly on ZnO/SiO_2 entrapped materials even after regenerating at 600°C for 3 h, without any detectable new peaks. Rapid growth of ZnO crystal, strong metal support interaction even solid reaction during regeneration are possible reasons for the poor regenerability of ZnO/γ-Al_2O_3 entrapped materials.

Table III. Comparison of regenerability of microfibrous entrapped supported ZnO and Sud-Chemie ZnO sorbent extrudates[a,*]

Sorbent	*ZnO Utilization, %*		
	Microfibrous entrapped ZnO/SiO_2	*Microfibrous entrapped $ZnO/\gamma\text{-}Al_2O_3$*	*Sud-Chemie extrudates (1-2mm)*
Fresh	67	65	31
3h@600°C in air**	60	8	21
1h@600°C in air**	57	12	13
3h@550°C in air**	44	15	4

[a] Bed configuration: 0.9 mL, 7mm (dia.) x 15 mm(thick).

* H_2S absorption was carried out at face velocity of 1.2 cm/s @ 2% H_2S and 98% H_2 (dry gas flow rate: 30 mL(STP)/min) at 400°C; ** Regeneration conditions.

Absorption/Regeneration Cycle Test

Figure 4 shows the cycle test results over microfibrous entrapped ZnO/SiO_2 at 400°C and face velocity of 1.2 cm/s. The breakthrough times (@ 1 ppmv H_2S detection limit) almost remained unchanged in 10 cycles at regeneration temperature of 600°C, and in 20 cycles at regeneration temperature of 500°C. The results suggest that ZnO/SiO_2 entrapped materials yield good thermal stability, even though they are regenerated many times. However, it is found that corrosion resistance of nickel fibers in air at higher temperature is a problem for regenerable use due to the oxidation of nickel fibers. The corrosion of nickel fibers during regeneration can be avoid by regenerating in hydrogen or other reducing environments. More recently, microfibrous carrier alternatives using corrosion resistant ceramic/glass fibers have been developed at Auburn University. The use of ceramic/glass fibers can extend the operating temperature range in oxidative environment up to 1200°C. This approach allows for continuous batch bulk H_2S removal from reformate streams while significantly increasing bed utilization efficiency and reducing overall system weight and volume. Figure 5 shows SEM micrographs of a typical sample of ceramic fiber entrapped 150-250 μm SiO_2 particulates.

H_2S Absorption of Microfibrous Entrapped ZnO/Carbon at Stack Temperature

Table IV shows the performance of microfibrous entrapped ZnO/Carbon for trace H_2S absorption from model reformate at stack temperatures (R.T. to 100°C) and face velocity of 1.7 cm/s in the presence of different H_2O content. Over 11 mm dia. × 3 mm thick) disc sorbent (0.29 mL), in 5% H_2O

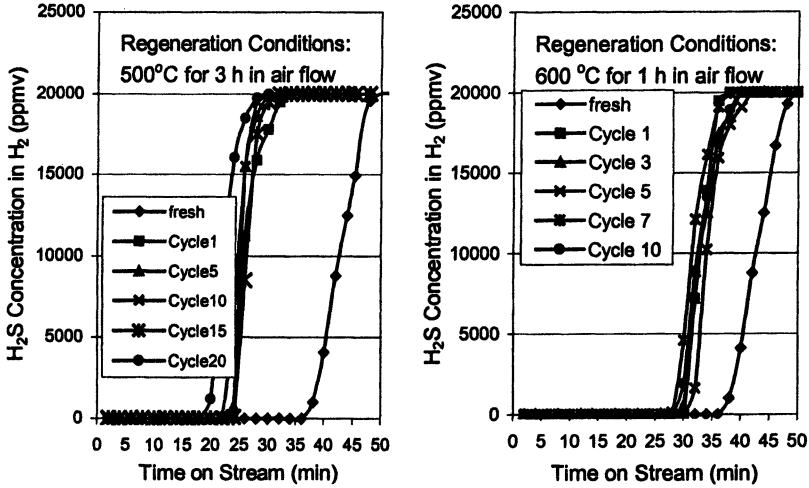

Figure 4. Absorption/regeneration cycle test results of microfibrous entrapped ZnO/SiO_2 sorbent. Adsorption with H_2S was carried out at 400°C and face velocity of 1.2 cm/s@ 2% H_2S and 98% H_2 (30 mL/min (STP).

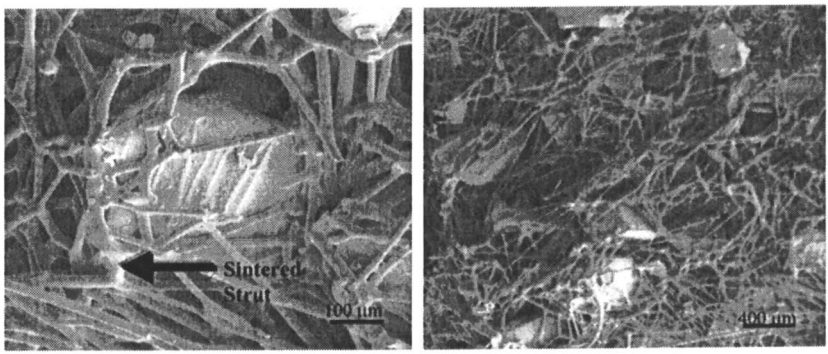

Figure 5. SEM micrographs of a typical sample of ceramic fiber entrapped SiO_2.

breakthrough time (@ 1ppmv H_2S detection limit) was from 7.8 h at 25°C to 9.5 h at 100°C with ZnO utilization from 30% to 39%. In 30% H_2O the disc sorbent provided breakthrough time of 8 h at 70°C and 32% of ZnO utilization.

Table IV. Performance of microfibrous entrapped ZnO/Carbon for H_2S absorption from model reformate at R.T. to 100°C in the presence of H_2O*

Sorbent	*Breakthrough Time (h)*	*ZnO Utilization (%)*
Microfibrous entrapped ZnO/Carbon (11 mm dia. × 3 mm thick)	9.5 @ 100°C in 5% H_2O	39
	8.7 @ 70°C in 5% H_2O	36
	7.8 @ 25°C in 5% H_2O	30
	8.0 @ 70°C in 30% H_2O	32

* Face velocity:1.7 cm/s @ 50 ppmv H_2S in model reformate (40% H_2, 10% CO, 20% CO_2, and 30% N_2); dry gas flow rate: 100 mL/min (STP).

This microfibrous entrapped ZnO/Carbon sorbent has been used as guard beds, for example, to protect PrOx CO catalyst at 150°C. In the presence of 50 ppmv H_2S in the feed gas, guard bed layers as thin as 3 mm in thickness placed in the front of the PrOx CO catalyst bed could maintain the activity/selectivity of the PrOx CO catalyst until breakthrough for H_2S occurred (*17*).

Figure 6 compares microfibrous entrapped ZnO/Carbon with several commercial sorbents for absorption with 50ppmv H_2S challenge in a model reformate at 70°C in 30% H_2O. At equivalent bed volume (0.29 mL, 11 mm dia. × 3 mm thick), 150-250 μm ZnO/Carbon entrapped materials provided 3-fold longer breakthrough times for H_2S than the high-temperature sorbent which is Sud-Chemie extrudates (1-2 mm) with a 67% reduction of sorbent loading. Four carbon-based sorbents (2-3 mm) for respiratory cartridges taken from different manufacturers were also checked versus our low-temperature sorbent, because they made low temperature H_2S absorption. In those cases, ZnO/Carbon entrapped materials provided about 3-fold longer breakthrough times for H_2S compared to packed beds of those four carbon-based 2-3 mm sorbents, even though their bed thickness was doubled.

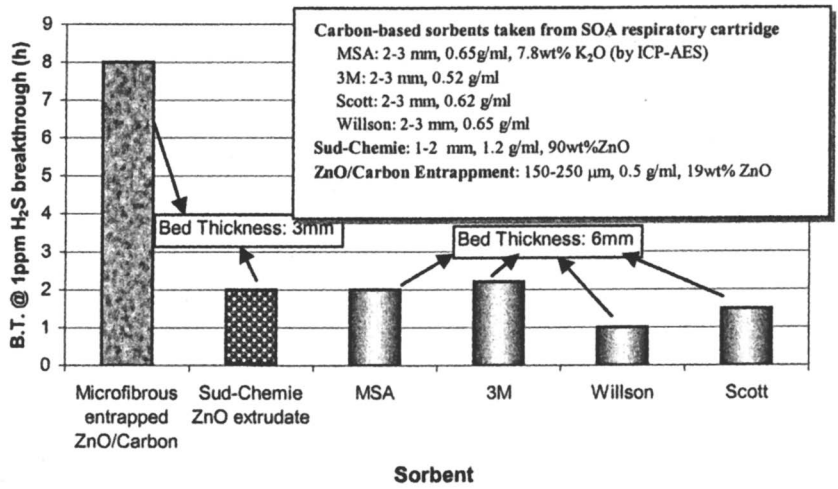

Figure 6. Comparison of microfibrous entrapped ZnO/Carbon with several commercially available sorbent particulates for absorption with 50 ppmv H_2S challenge in a model reformate in 30% at 70°C and face velocity of 1.7 cm/s (100 mL/min, STP).

Composite Bed: Optimization of Microfibrous Entrapped Particle Solid

The polishing sorbent concept allows opportunities for higher absorption capacity design by incorporating microfibrous sorbent composite as a polishing sorbent layer to back up a packed bed that suffers from high intraparticle mass transfer and low contacting efficiency.

A composite bed consisting of packed bed of 1-2 mm SudChemie ZnO extrudates followed by microfibrous entrapped ZnO/SiO_2 polishing sorbents has been demonstrated for H_2S removal from a H_2 fuel stream. Figure 7 shows the breakthrough curves for a 2 vol% H_2S challenge in H_2 in single and composite beds at 400°C and a face velocity of 1.2 cm/s. Two single beds, 7 mm (dia.) × 3 mm (thick) microfibrous entrapped ZnO/SiO_2 (A) and 7 mm (dia.) ×7 mm (high) packed bed of 1-2 mm Sud-Chemie ZnO sorbent extrudates (B), provided

breakthrough times (@1 ppmv H_2S detection limit) of 5 min and 28 min, respectively. The breakthrough curve with small particulates (ZnO/SiO_2) alone is very sharp. But the breakthrough curve in packed bed with large particulates (B) is very sigmoidal. When the polishing sorbent was placed behind the packed bed (B+A), the outlet from the packed bed B, where the H_2S concentrations increased very slowly with time in stream after the breakthrough point in bed B, was encountered immediately with the high contacting efficiency polishing sorbent A. As a result of more efficient use of sorbent, breakthrough time of composite bed is extended to 52 min. The breakthrough with the sharpness of the curve is also indicative of the polishing sorbent. Similar absorption behavior for trace H_2S removal from H_2 fuel stream has also been achieved at stack temperatures in a composite bed. The conjecture to explain this behavior might be due to the fact that the integral of the effluence from the first bed integrated to the total breakthrough time will be equal to the breakthrough time of the polishing sorbent multiplied by the challenge concentration (Area 1 as shown in Figure 7). This idea was early expressed as a "Bed Depth Service Time Equation" by Adams and Bohart (18). This equation is used to describe the packed beds of particles with strong physical adsorption; however, the equation does not take the residence time of the bed into account. Cahela and Tatarchuk (19) accounted for the residence time of the bed and obtained the concentration breakthrough equation to depict this conjecture. The concentration breakthrough equation was developed for a bed with a polishing filter under the assumption that a polishing filter will absorb the effluents from the front bed until the breakthrough time of the polishing filter and resulted in the equal areas behavior of a polishing sorbents.

Conclusion

The growing demand in small, efficient, lightweight fuel processing systems utilizing commercial-grade liquid hydrocarbon fuels makes the microfibrous materials attractive for commercial applications. A highly void, tailorable sintered-nickel-fiber carrier can be fabricated via wet layer paper-making process. By entrapping and isolating ZnO/support with particulate size of 150-250 μm into the microfibrous network, the low pressure drop can be maintained while withstand considerable shaking, and avoiding by-passing. A carrier consisting of 2 vol% Ni fibers was utilized to entrap 150-250 μm ZnO/SiO_2 sorbents for H_2S removal. The smaller size of ZnO sorbent enhances the intraparticle mass transfer and yields high-log removal, but in turn produces high pressure drop. The nano-dispersed nature of ZnO combined with the use of small support particulated not only promotes high ZnO utilization, high contacting efficiency, and high accessibility of ZnO, but also facilitates the regeneration in air at 500-600°C compared to that of the packed bed of 1-2 mm commercial extrudates. Moreover, the use of the microfibrous carrier allows a large number

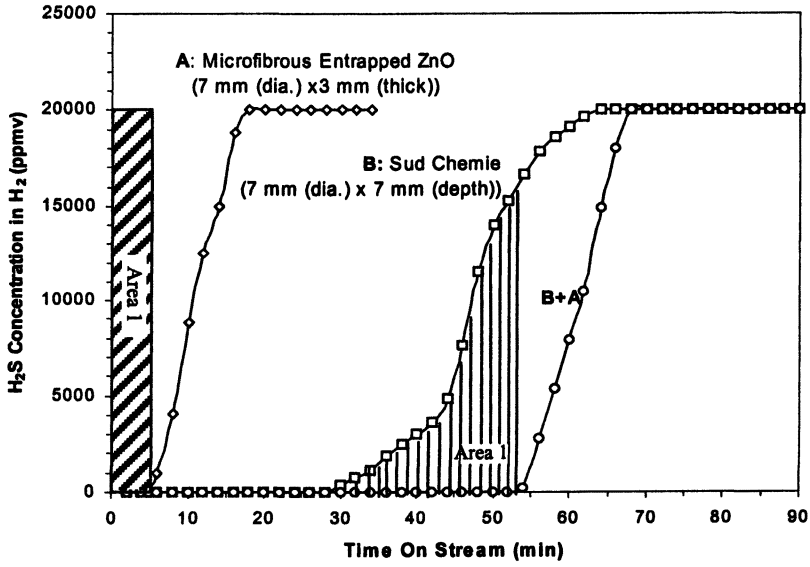

Figure7. Performance of single and composite beds for H_2S absorption from 2% H_2S and 98% H_2 at 400°C with a face velocity of 1.2 cm/s (30 mL/min, STP).

of absorption/regeneration cycles due to their high thermal stability. This approach synergistically combines the high volume loading of packed beds and the high contacting efficiency of small particulates, which allows a significant increase in bed utilization, contacting efficiency, and reduction in overall system weight and volume. This approach towards small-scale regenerable continuous batch fuel processing in PEMFC applications is commercially feasible by using microstructured particulate carriers.

Acknowledgements

The authors are grateful to Dr. Thomas E. Albrecht-Schmitt for his assistance in performing the XRD. We also would like to acknowledge Drs. Wenhua Zhu, Don Cahela, B.K. Chang, and Mr. Dwight Cahela, all of the Center for Microfibrous Materials Manufacturing (CM^3) at Auburn University, for their technical assistance and helpful discussions.

References

1. Tatarchuk, B. J.; Rose, M. F.; Krishnagopalan, A.; Zabasajja, J.N.; Kohler, D. U.S. Patent 5,304,330, 1994; U.S. Patent 5,080,963, 1992.
2. Overbeek, R. A.; Khonsari, A. M.; Chang, Y.-F.; Murrell, L. L.; Tatarchuk, B. J.; Meffert, M. W. U.S. Patent 6,231,792, 2001.
3. Tatarchuk, B. J. U.S. Patent 5,096,663, 1992; U.S. Patent 5,102,745, 1992.
4. Cahela, D. R.; Tatarchuk, B. J. *Catal. Today* **2001**, *69*, 33-39.
5. Marrion, C. J.; Cahela, D. R.; Ahn, S.; Tatarchuk, B. J. *J. Power Sources* **1994**, *47*, 297-302.
6. Kohler, D. A.; Zabasajja, J. N.; Krishnagopalan, A.; Tatarchuk, B. J. *J. Electrochem. Soc*. **1990**, *137(1)*, 136-141.
7. Ahn, S.; Tatarchuk, B. J. *J. Appl. Electrochem*. **1997**, *27*, 9-17.
8. Meffert; M. W. Ph.D. thesis, Auburn University, Auburn, AL, 1998.
9. Harris, D. K.; Cahela, D. R.; Tatarchuk, B. J. *Composites, Part A: Applied Science and Manufacturing* **2001**, *32A*(8), 1117-1126.
10. Chang, B. K.; Lu, Y.; Tatarchuk, B. J. Materials Solutions Conference and Exposition, Columbus, Ohio, USA, Oct. 18-21, 2004.
11. Karanjikar, M. R.; Lu, Yong; Chang, B. K.; Tatarchuk, B. J. Proceeding of the 41st Power Sources Conference, Philadelphia, Pennsylvania, United States, June 14-17, 2004, p 231-234
12. Trubac, R. E.; Dautzenberg, F. M.; Griffin, T. A.; Paikert, B.; Schmidt, V. R.; Overbeek, R. A. *Catal. Today* **2001**, *69*, 17-24.

13. Zawodzinski, T.; et. al. Proceedings of the Annual National Laboratory R&D Meeting, Oak Ridge, Tennessee, June 6-8, 2001.
14. Song, C. *Catal. Today* **2002**, *77*(1-2), 17-49.
15. Cervi, M.; Hoffman, D. 2nd DOD Diesel Fuel Reforming Coordination Meeting, Fort Belvoir, Virginia, Dec. 2001.
16. Twigg, M. V. *Catalyst Handbook* (2nd ed.); Wolfe: London, 1989; pp.209.
17. Chang, B. K.; Tatarchuk, B. J. AIChE 2003 National meeting, San Francisco, CA, November 16-21, 2003, 170a.
18. Bohart, C. S.; Adams, E. Q. *J. Am. Chem. Soc.* **1920**, *42*, 523-544.
19. Cahela D. R.; Tatarchuk B. J. AIChE 2003 National meeting, San Francisco, CA, November 16-21, 2003, 138c.